Asian Journal of Chemistry Vol. 14, No. 2 (2002), 1009–1026

Evaluation of Different Grades of Granular Activated Carbon Adsorbents for Scavenging Priority Pollutants from Wastewater

S.S. SHASTRI* and M.K.N. YENKIE†
Department of Applied Chemistry
Yashwantrao Chavan College of Engineering, Wanadongri, Hingna Road, Nagpur, India

Increasing environmental awareness and concern have expanded the role of powdered activated carbon (PAC) and granular activated carbon (GAC) adsorbents in scavenging the soluble, chemically stable and biologically non-degradable pollutants from industrial and domestic wastewater. In the present investigation adsorbents prepared from bituminous coal, namely, Filtrasorb-100 (F-100), Filtrasorb-200 (F-200), Filtrasorb-300 (F-300), Filtrasorb-400 (F-400) and coconut shell based carbons LCK and RRL were evaluated for their efficiency and performance in scavenging pollutants from water. Aqueous solution of *m*-nitrophenol was used as adsorbate. These GAC samples were subjected to Proximate and Ultimate Analysis, Pore Size Distribution (PSD), Scanning Electron Microscopy (SEM) and Fourier Transform Infrared Spectroscopy (FTIR). Results show that the source material used for preparation of GAC has significant effect on its pore structure, surface texture, resistance to fragmentation and adsorption capacity. Bituminous coal based carbons show high ash content, a rough surface having lot of cracks and irregular protrusions, high pore volume and a widely dispersed pore structure. In contrast, the coconut shell based GAC samples have low ash content, low pore volume and exhibit uniformly dispersed finer pores, which are well connected by solid mass. FTIR spectra show the presence of various carbon-oxygen complexes on the granular activated carbon surface, which makes the surface slightly polar. The effect of physico-chemical parameters associated with the adsorbent on the adsorption equilibrium and adsorbate removal rate was also studied. Adsorption equilibrium and kinetic experiments were carried out in a batch reactor. The obtained results showed that bituminous coal based carbons have higher adsorption capacity for phenols as compared to the coconut shell based carbons.

Key Words: Adsorption, Activated carbon, Pore size distribution, Scanning Electron microscopy, FTIR, Phenols, Adsorption equilibrium, Adsorption kinetics, Wastewater.

INTRODUCTION

Complete removal or reduction of concentration of hazardous organic chemicals to an acceptable limit has become a major concern of advanced water and

†Reader in Chemical Technology, Laxminarayan Institute of Technology, Nagpur University, Nagpur-440 010, India.

wastewater treatment technology. The conventional biological and physical treatment processes are not always capable of removing these substances adequately. In order to comply with the effluent limits imposed by environmental protection agencies, a broad range of treatment processes are in application. In recent years adsorption on activated carbon has proved promising in removing refractory organic compounds at tertiary treatment level. The availability of a wide variety of activated carbons in several countries, its versatility as a liquid phase adsorbent[1] and the recent inroads into the regeneration of spent GAC samples for many cycles[2] has boosted its application in wastewater treatment technology.

The adsorption phenomenon is largely governed by the physico-chemical characteristics of the adsorbent and adsorbate. However, interpretation of the adsorptive behaviour based on the total adsorbent surface area alone is incomplete, as carbons having equal weights and equal total surface areas when prepared by different methods exhibit different adsorptive characteristics. Some of the adsorptive properties can be explained by differences in relative pore size distributions, but a more important consideration is the difference in surface properties of the carbons. The chemical nature of the surface functional groups present on the activated carbon surface depends on the activation procedure employed in its manufacture or regeneration process.

In the present investigation, adsorption potential of different grades of granular activated carbons prepared from different sources has been studied. Commercially available bituminous coal based activated carbons namely Filtrasorb-100 (F-100), Filtrasorb-200 (F-200), Filtrasorb-300 (F-300), Filtrasorb-400 (F-400), and coconut shell based samples LCK and RRL were used as adsorbents. These samples were procured directly from the manufacturers and other sources (Table-1) and were subjected to proximate and ultimate analysis, phenol-BET surface area measurement, pore size distribution measurement, scanning electron microscopy (SEM) and FTIR spectroscopy to determine the physical and chemical nature of the GAC surface. The aqueous phase adsorption behaviours of these adsorbents were compared by studying the adsorption equilibrium and removal rate of *m*-nitrophenol (MNP) from its aqueous solution.

Granular activated carbon: Granular activated carbon is a solid of indefinite structure. It is highly porous in character and its pore and surface characteristics depend on the source material used for its preparation and the activation process[3, 4]. The adsorbents presently used all over the world for various purposes have an internal surface area greater by several orders of magnitude than the external surface area, located predominantly in micropores. The large internal surface area is produced during activation process where part of the parent solid is removed by controlled burning of carbon or by thermal decomposition where the loss of volatile components leads to the development of a highly heterogeneous porous structure and surface characteristics. However, this enormous surface area is only restricted to those cavities which have an opening to the exterior of the granule and not the sealed pores. The electron micrographs clearly show the presence of macro-, meso- and micropores. Adsorption is rapid in the macropores and a portion of the adsorbate finds its way into the micropores

TABLE-1
PHYSICO-CHEMICAL PROPERTIES OF VARIOUS GRANULAR ACTIVATED CARBON (GAC) SAMPLES USED

Name	F-100*	F-200*	F-300*	F-400*	LCK†	RRL‡
Source	Biuminous coal	Bituminous coal	Bituminous coal	Bituminous coal	Coconut shell	Coconut shell
N_2-BET area	841 m^2/g	825 m^2/g	970 m^2/g	998 m^2/g	1025 m^2/g	900 m^2/g
Particle density	0.7382 g/cm^3	0.8580 g/cm^3	0.7303 g/cm^3	0.7950 g/cm^3	0.7530 g/cm^3	0.8020 g/cm^3
True density	2.079 g/cm^3	2.267 g/cm^3	2.100 g/cm^3	2.308 g/cm^3	2.010 g/cm^3	2.110 g/cm^3
Pore volume	0.549 cm^3/g	0.724 cm^3/g	0.850 cm^3/g	0.825 cm^3/g	0.671 cm^3/g	0.379 cm^3/g
Porosity	0.26	0.53	0.64	0.65	0.33	0.30
Proximate analysis (%)						
Moisture	5.4	10.5	5.3	1.9	6.8	5.5
Ash	5.5	5.8	5.4	6.1	0.6	0.9
Volatile matter	2.7	5.6	1.7	2.7	3.8	5.0
Fixed carbon	86.4	78.1	87.6	89.3	88.8	88.6
Mineral matter	6.05	6.38	5.94	6.71	0.66	0.99
Ultimate analysis (%)						
C	95.32	93.80	97.63	96.04	92.94	94.56
H	0.27	0.49	0.18	0.29	0.41	0.44

* Filtrasorb grades of GAC are manufactured by Calgon Corporation, Pittsburgh, A.C. Division, Pa. 15230, U.S.A.
† LCK carbon is supplied by National Carbon Co., Union Carbide Corporation Production Division, New York, NY 10017, U.S.A.
‡ RRL grade of GAC was prepared at Indian Institute of Chemical Technology, Hyderabad, India

over a delayed period of time. This implies that the adsorption phenomenon is rapid at start but slows down with time.

Pore size distribution (PSD) measurement of a given granular activated carbon sample provides the information on the adsorbent structure. The internal surface area of activated carbons, generally greater than 400 m^2/g, is mostly located in the micropores having pore diameter less than 20 Å. Whether a specific molecule is adsorbed or not in a pore is determined by the size of adsorbate as well as the pore. The pore size distribution (PSD) results are presented in Figs. 1 and 2. PSD

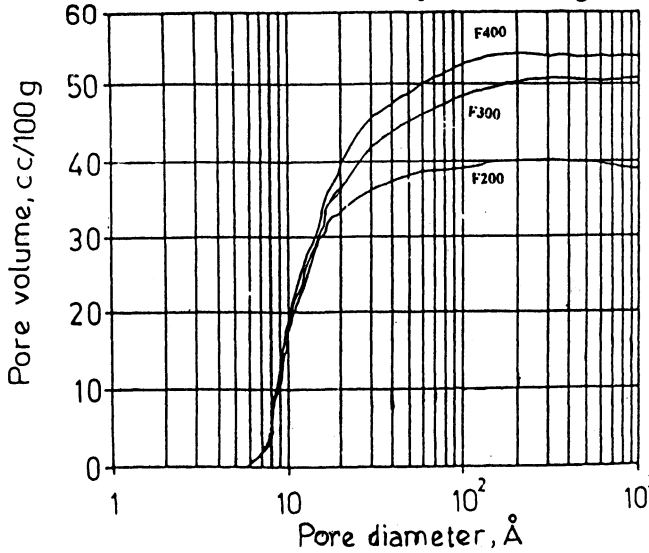

Fig. 1. Pore size distribution of GAC samples

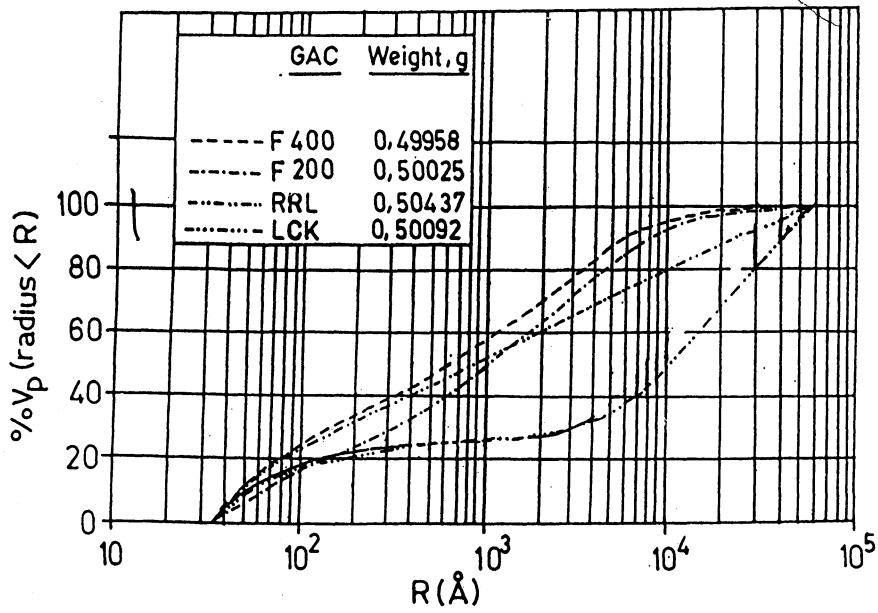

Fig. 2. Pore size distribution of GAC samples

analyses of the GAC samples shown in Fig. 1 were carried out on a Carlo Erba Mercury Porosimeter (Courtesy M/s Alchemie, Bombay, India). As can be seen from Fig. 1, the Carlo Erba Mercury Porosimeter could not detect pores below 35 Å, whereas, PSDs of F-200 and F-400 carbons (Fig. 2, supplied by the manufacturer) clearly show the existence of pore diameters as low as 6.5 Å. Thus the surface area calculated from pore size distribution is likely to throw more light on the presence of pores of lower diameters and their abundance. The surface area can be calculated by knowing the volume of mercury penetrating into the pore space of a given diameter using the formula[5].

$$\text{Surface area} = \frac{4\ (\text{volume of Hg})}{\text{diameter of pore}}$$

The surface areas calculated using the above relation are summarised in Table-2.

TABLE-2
ADSORBENT SURFACE AREA IN m^2/g FROM PSD MEASUREMENTS

GAC	F-100	F-200	F-300	F-400	RRL	LCK
Carlo Erba*	—	17.56	—	48.07	31.20	16.56
From Fig. 3	—	825	—	998	—	—
N_2-BET†	841	825	970	998	900	1025

* Information provided by M/s Alchemie, Mumbai, India.
†Information provided by the manufacturers.

Since the surface area calculated using the pore size distribution results obtained on Carlo Erba mercury porosimeter is only around 2–5% of surface area obtained from Fig. 2 and N_2-BET method, it may be inferred that 95–98% of the adsorbent surface area exists in pores below 35 Å in radius, which explains the slow approach to adsorption equilibrium following an initial rapid uptake period[6]. Surface area for these GAC samples has also been determined using adsorption isotherms of *m*-nitrophenol and the results have been discussed at a later stage.

Proximate and ultimate analysis of adsorbents: These adsorbents were subjected to proximate and ultimate analysis and the obtained results are summarised in Table-l. The moisture content of bituminous coal based sample Filtrasorb-200 was highest at 10.5% and that for Filtrasorb-400 was lowest at 1.9%. The bituminous coal based carbons F-100, F-200, F-300 and F-400 have much higher ash (5.4–6.1%) and mineral matter (5.9–6.7%) content. The coconut shell based samples RRL and LCK show moisture content around 6%. The fixed carbon content for all samples was found to be around 88–90% except for Filtrasorb-200, which had fixed carbon content of only 78.1%. The coconut shell based carbons show lower ash content. Their high carbon and low hydrogen percentage, as evident by the ultimate analysis, supports the observation that these carbons are structurally very hard and show a very high resistance to fragmentation. The carbon, ash, moisture and mineral matter content reflects itself in the crystalline and porous structure of the adsorbent particle as samples having higher

ash and mineral content are likely to be more fragile as compared to the samples having very low ash content.

Scanning electron microscopy and FTIR spectroscopy: The SEM micrographs show that GAC samples prepared from different sources have significantly different pore structure and surface characteristics. The bituminous coal based samples F-100, F-200, F-300 and F-400 show a layered, loosely packed structure with a lot of cavities, cracks, irregular protrusions and widely dispersed pores. The relative high ash and mineral matter content of these samples (Table-1) may be causing the loose packing as can be seen form tiny particulate material in the micorgraphs. The proximate analysis indicates a very high moisture content in F-200 sample, which means that the water molecules must be getting entrapped in these cracks and layers. In comparison, the coconut shell based RRL and LCK samples indicate a more compact structure with uniformly distinguished pores well connected by solid mass. They show few fines as indicated by their high carbon and low ash content. The low pore volume and high particle density of the RRL carbon is justified by its pore size distribution measurement and SEM micrograph. These differences in the structure of various adsorbents make them suitable or unsuitable for gas or liquid phase adsorption applications. Adsorbents with widely distributed pores having large number of cavities and cracks are generally suitable for liquid phase adsorption studies, whereas those having fine and regular pores are more suitable for gas phase adsorption operations[2].

Fourier Transform Infrared Spectra: FTIR spectra of adsorbent samples in a KBr matrix[7] was recorded between 4000–400 cm^{-1} at room temperature. The FTIR spectra clearly show the various groups present on activated carbon surface. The predominant presence of free phenolic —OH stretch vibration around 3500 cm^{-1} is visible in all GAC samples[7-9]. The bands around 3000–2900 cm^{-1} are probably due to the symmetric and asymmetric C—H stretch vibrations particularly at 2808 cm^{-1}, which were present in coconut shell based samples and were not observed in bituminous coal based samples which can be attributed to a hydrogen bonding in low ash content samples. The spectra below 1000 cm^{-1} were marked by the noisy spectrum. GAC sample F-100 shows peaks around 1622 cm^{-1} to 1582 cm^{-1} which corresponds to the vibrations of C=O in the quinone configuration. The asymmetric O=C=O stretch vibration of CO_2 adsorbed in pores of adsorbent are represented by bands around 2361 cm^{-1} and 2336 cm^{-1}. The C—O stretch vibration (phenol, $—COO^-$) around 1200 cm^{-1} were also observed in the adsorbents.

The FTIR spectra of F-200 also show the presence of C=O vibrations in the quinone configuration. The peaks at 1074 cm^{-1} probably indicate the moisture inclusions in between the layers as F-200 had about 10.5% moisture content. Filtrasorb-300 shows nearly identical infrared spectra as observed for the F-200. The quinone C=O group is configured strongly in this sample. FTIR peaks around 1628 cm^{-1} and 2364 cm^{-1} are seen in the spectra of F-400 samples; the band at 1629 cm^{-1} represents H—O—H bonding.

There appears to be remarkable difference in the FTIR spectrum of RRL and LCK samples although both are coconut shell based carbons which may be due to the activation process employed for their preparation. The FTIR spectrum of

LCK sample shows that the quinone ring or H—O—H linkage is completely missing but new conjugated C=O configuration seems to form. The band around 1737 cm^{-1} may be due to the C=O stretch vibrations from CHO, COO^- or δ lactone group. The RRL sample also appears to contain C—O, C=O groups on its surface represented by bands around 1527 cm^{-1}, 1469 cm^{-1} and 1430 cm^{-1}. It can be thus summarised that the FTIR spectrum shows predominant presence of free —OH on stretch vibration of phenol around 3500 cm^{-1} in all GAC samples[10] and following other groups:

- Asymmetric and symmetric C—H stretch vibrations around 2808 cm^{-1} for all GAC samples
- The asymmetric O=C=O stretch vibration of CO_2 adsorbed in pores around 2347 cm^{-1}
- C—O stretch vibration (phenol, COO^-) around 1200 cm^{-1} in these carbons
- C=O stretch vibrations around 1735 cm^{-1}
- Methylene vibrations around 1644 cm^{-1}
- The spectra below 1000 cm^{-1} noisy spectrum.

EXPERIMENTAL

Adsorbate concentration in solutions was measured by UV spectroscopy by measuring the optical density of the component at its wavelengths of maximum absorbance. The UV absorption measurements were carried out on a GBC UV/VIS 911A spectrophotometer (GBC Scientific Equipments, Melbourne, Victoria, Australia) using matched 1 cm path length cuvettes. The adsorbate, *m*-nitrophenol, had very strong absorption bands at 280 nm with high molar extinction coefficient values (ε). This naturally served as a very simple, reliable and rapid method for analysing the adsorbate concentration in water. Regression analysis of the experimental data of adsorbate concentration *vs.* optical density for the standard Beer's law plot was carried out to evaluate the molar extinction coefficients (ε) value given below[2].

Adsorbate	Symbol	m.w.	Water solubility (mol/L at 30°C)	λ_{max}	ε (nm)
m-Nitrophenol	MNP	139.11	0.3617	280	1317

The experimental arrangement for carrying out both the equilibrium as well as the kinetic runs varied considerably. For adsorption equilibrium studies, a one-litre round bottom flask containing 500 mL of distilled water was immersed in the thermostat bath. The contents were constantly stirred at 800 ± 50 RPM and allowed to attain the temperature of bath, which usually took around 25 to 30 minutes. The impeller used to stir the experimental solutions was fabricated out of a 6 mm glass rod having a simple teflon or nylon paddle fitted to its lower end. The information available in literature[11] states that the ratio of length of paddle to the diameter of the reactor containing the solution to be stirred, should lie between 0.20 to 0.50. In this work this ratio was fixed at 0.325, *i.e.*, the paddle length was kept at 5.0 cm. It has also been suggested that the ratio of width of

the blade to its length should lie between 1/4 to 1/6. In this work, this has been arbitrarily fixed at 0.30.

Adsorption equilibrium studies

After the desired temperature was reached, a calculated quantity of the stock solution, measured with the help of a measuring pipette, was introduced into the distilled water. The solution was allowed to mix thoroughly to achieve the desired concentration and the same quantity of the resulting solution was pipetted out to keep the final solution volume at 500 mL. This pipetted solution was used for determination of initial adsorbate concentration. 0.250 ± 0.001 g of the adsorbent sample was now introduced into the solution and stirring was maintained at 800 ± 50 rpm. The time of addition of GAC was noted. Stirring was continued till the concentration of the aqueous phase showed no detectable change in UV absorbance. From preliminary experiments it was observed that the adsorbate uptake profile was independent of stirrer speed above 600 rpm[12] and the equilibrium was attained in above 3.5 to 4 h. As a precautionary measure, experiments were continued for 5 h. Some of the experiments were carried out over a prolonged period of time where no significant difference was noticed in the adsorbate concentration. Some of the points on the isotherm were also tested for their reproducibility. Such an experiment enables one to obtain equilibrium data for an adsorbent/adsorbate system at a given temperature. Experiments were carried out by varying the concentration of the adsorbate in solution to obtain equilibrium data which would help in arriving at the adsorption isotherm. The (GAC/adsorbate solution volume) ratio was kept constant at 0.250 g/500 mL in all equilibrium experiments. The adsorption equilibrium data are reported in Tables 3 and 4.

Adsorption kinetics studies

For adsorption kinetic studies, the experimental unit was a cylindrical batch reactor of 7 L capacity. It was made up of plexi glass and was fitted with eight baffles at 45° each. The adsorbent-adsorbate system was stirred by a two-bladed impeller having length 7 cm and breadth 1.5 cm. Experimental solution for kinetic runs was 4 L in volume and was prepared by adding appropriate amount of stock solution into boiled and cooled distilled water. 2.0000 ± 0.0001 g of a given GAC sample was introduced into the solution at a given instant of time. At desired interval, 5 mL of experimental solution was withdrawn with the help of a syringe and the concentration of the adsorbate in the aqueous phase was estimated by UV analysis. The obtained adsorption kinetic data are reported in Table-5.

RESULTS AND DISCUSSION

Adsorption isotherms: The adsorption isotherms obtained in the present work fall under typical Type I favourable isotherm[13]. The equilibrium data was analysed for the validity of Langmuir and B.E.T. isotherm equations. Since the concentrations of pollutants in water and wastewater after primary and secondary treatment are micromolar, it is of interest to examine the Langmuir and B.E.T.

TABLE-3
EXPERIMENTAL ADSORPTION EQUILIBRIUM DATA OF *m*-NITROPHENOL ON DIFFERENT GRADES OF GAC

T = 30°C; pH = 6.9–7.0, GAC particle size = 12 × 16

No.	GAC: F-100				GAC: F-200				GAC: F-300			
	C_0, mol/L	C_e, mol/L	Q_e, mol/g	C_e/Q_e	C_0, mol/L	C_e, mol/L	Q_e, mol/g	C_e/Q_e	C_0, mol/L	C_e, mol/L	Q_e, mol/g	C_e/Q_e
1	0.000082	0.000029	0.000053	0.547170	0.000103	0.000028	0.000075	0.373333	0.000105	0.000024	0.000081	0.298420
2	0.000145	0.000052	0.000093	0.559140	0.000208	0.000049	0.000159	0.308176	0.000213	0.000041	0.000172	0.241042
3	0.000396	0.000068	0.000328	0.207317	0.000398	0.000063	0.000335	0.188060	0.000421	0.000063	0.000358	0.176109
4	0.000604	0.000131	0.000473	0.276956	0.000611	0.000126	0.000485	0.259794	0.000608	0.000103	0.000505	0.202861
5	0.000745	0.000159	0.000586	0.271331	0.000811	0.000149	0.000662	0.225076	0.000818	0.000126	0.000692	0.182723
6	0.000946	0.000244	0.000702	0.347578	0.001015	0.000234	0.000781	0.299616	0.001026	0.000208	0.000818	0.253573
7	0.001183	0.000419	0.000764	0.548429	0.001197	0.000386	0.000811	0.475956	0.001227	0.000294	0.000933	0.314869
8	0.001435	0.000667	0.000768	0.868490	0.001421	0.000583	0.000838	0.695704	0.001439	0.000448	0.000991	0.451892
9	0.001647	0.000882	0.000765	1.152941	0.001628	0.000784	0.000844	0.928910	0.001614	0.000604	0.001010	0.598023
10	0.001811	0.001044	0.000767	1.361147	0.001821	0.000944	0.000877	1.076397	0.001846	0.000824	0.001022	0.805656
11	0.002023	0.001249	0.000774	1.613695	0.002035	0.001152	0.000883	1.304643	0.402111	0.001072	0.001039	1.031713
12	0.002198	0.001430	0.000768	1.861979	0.002185	0.001301	0.000884	1.471719	0.002208	0.001191	0.001017	1.171098

No.	GAC : F 400				GAC : RPL				GAC : LCK			
	C_0, mol/L	C_e, mol/L	Q_e, mol/g	C_e/Q_e	C_0, mol/L	C_e, mol/L	Q_e, mol/g	C_e/Q_e	C0, mol/L	C_e, mol/L	Q_e, mol/g	C_e/Q_e
1	0.000107	0.000022	0.000085	0.260246	0.000101	0.000026	0.000075	0.346320	0.000105	0.000026	0.000079	0.328731
2	0.000135	0.000025	0.000110	0.227277	0.000112	0.000019	0.000093	0.205128	0.000216	0.000047	0.000169	0.277701
3	0.000406	0.000060	0.000346	0.173265	0.000383	0.000057	0.000326	0.175649	0.000407	0.000060	0.000347	0.172795
4	0.000608	0.000110	0.000498	0.220863	0.000578	0.000101	0.000477	0.212469	0.000610	0.000111	0.000499	0.222293
5	0.000817	0.000128	0.000689	0.185910	0.000782	0.000135	0.000647	0.208526	0.000810	0.000130	0.000680	0.191058
6	0.001027	0.000191	0.000836	0.228417	0.000998	0.000202	0.000796	0.253896	0.001014	0.000207	0.000807	0.256655
7	0.001232	0.000303	0.000929	0.326202	0.001182	0.000326	0.000856	0.380819	0.001229	0.000302	0.000927	0.325864
8	0.001434	0.000440	0.000994	0.442631	0.001406	0.000469	0.000937	0.500547	0.001417	0.000447	0.000970	0.460957
9	0.001615	0.000602	0.001013	0.594035	0.001591	0.000623	0.000968	0.643479	0.001620	0.000632	0.000988	0.639785
10	0.001831	0.000750	0.001081	0.694041	0.001805	0.000836	0.000969	0.862612	0.001822	0.000832	0.000990	0.840462
11	0.002067	0.000984	0.001083	0.908868	0.001982	0.001009	0.000973	1.036946	0.002086	0.001083	0.001003	1.080114
12	0.002231	0.001138	0.001093	1.041314	0.002192	0.001201	0.000991	1.212397	0.002232	0.001214	0.001018	1.192307

TABLE-4
ADSORBATE REMOVAL RATE DATA OF *m*-NITROPHENOL ON VARIOUS GAC SAMPLES.

GAC: 12 × 16 mesh, T = 30°C, pH = 6.9–7. 1

GAC		F-100		F-200		F-300		F-400		LCK		RRL	
No.	T, min	C_t, mol/L	C_t/C_0	Ct, mol/L	C_t/C_0	Ct, mol/L	C_t/C_0	Ct, mol/L	C_t/C_0	Ct, mol/L	C_t/C_0	Ct, mol/L	C_t/C_0
1	0	0.000172	1.0000	0.000171	1.0000	0.000172	1.0000	0.000169	1.0000	0.000168	1.0000	0.000167	1.0000
2	5	0.000157	0.9128	0.000153	0.8947	0.000148	0.8605	0.000142	0.8402	0.000147	0.8750	0.000148	0.8862
3	10	0.000136	0.7907	0.000131	0.7661	0.000124	0.7209	0.000124	0.7337	0.000130	0.7738	0.000132	0.7904
4	20	0.000117	0.6802	0.000113	0.6608	0.000109	0.6337	0.000110	0.6509	0.000117	0.6964	0.000118	0.7066
5	30	0.000101	0.5872	0.000098	0.5731	0.000094	0.5465	0.000100	0.5917	0.000103	0.6131	0.000104	0.6228
6	40	0.000090	0.5233	0.000088	0.5146	0.000082	0.4767	0.000085	0.5030	0.000090	0.5357	0.000091	0.5449
7	60	0.000075	0.4360	0.000072	0.4211	0.000065	0.3779	0.000072	0.4260	0.000077	0.4583	0.000078	0.4671
8	90	0.000063	0.3663	0.000062	0.3626	0.000049	0.2820	0.000060	0.3550	0.000062	0.3715	0.000070	0.4192
9	120	0.000055	0.3198	0.000054	0.3158	0.000041	0.2407	0.000048	0.2840	0.000053	0.3149	0.000062	0.3713
10	150	0.000050	0.2915	0.000046	0.2690	0.000035	0.2035	0.000037	0.2189	0.000041	0.2452	0.000050	0.2994
11	180	0.000047	0.2730	0.000043	0.2515	0.000033	0.1919	0.000030	0.1775	0.000037	0.2202	0.000037	0.2216
12	210	0.000043	0.2500	0.000042	0.2456	0.000032	0.1860	0.000027	0.1598	0.000031	0.1845	0.000035	0.2096
13	240	0.000042	0.2442	0.000038	0.2222	0.000031	0.1802	0.000027	0.1598	0.000030	0.1786	0.000034	0.2036
14	270	0.000042	0.2442	0.000038	0.2222	0.000031	0.1802	0.000026	0.1538	0.000030	0.1786	0.000034	0.2036

isotherm equations in the very low adsorbate concentration range such as those studied in this investigation. The B.E.T. equation is:

$$\frac{C_e}{Q_e(C_s - C_e)} = \frac{1}{Q°Z} + \frac{(Z-1)}{Q°Z}\frac{C_e}{C_s} \quad (1)$$

In the present work $C_s \gg Ce$ and $(Z - 1) = Z$; therefore

$$\frac{C_e}{Q_eC_s} = \frac{1}{Q°Z} + \frac{C_e}{Q°C_s} \quad (2)$$

which reduces to the Langmuir expression,

$$(C_e/Q_e) = (1/Q°b) + (C_e/Q°), \quad \text{where } b = (Z/Cs) \quad (3)$$

Thus at micromolar concentration range of solute the two isotherms give same results which were observed in this work. Langmuir isotherm plots were therefore carried out for all the adsorbate-adsorbent systems. The isotherms are depicted in Figs. 3 and 4. These plots also show the Langmuir equation obtained by linear

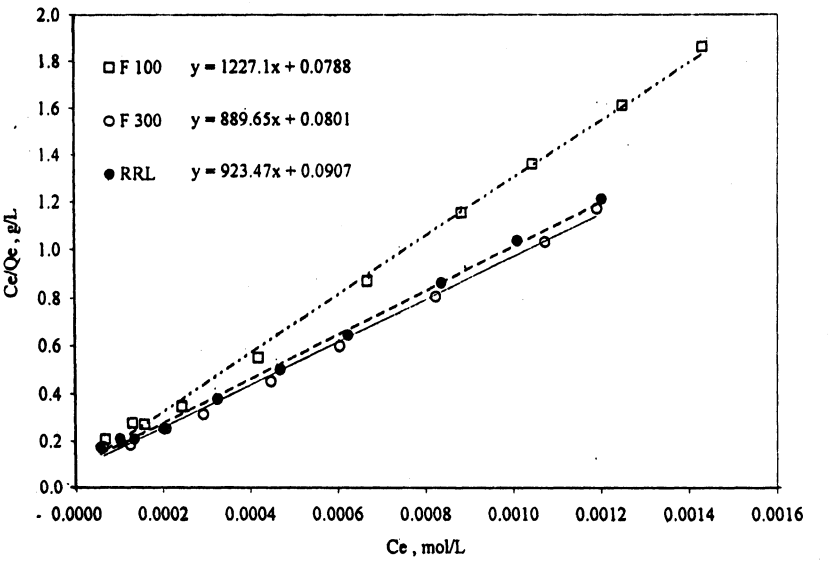

Fig. 3. Langmuir adsorption isotherms of *m*-nitrophenol on different grades of GAC

regression of the data. The regression coefficient values were above 0.98 indicating a very good linear fit in all the cases. The monolayer capacity 'Q°' can be used to determine the surface area of the adsorbent using the relation

$$S = Q°NA \quad (4)$$

where, N = Avogadro number,

A = cross-sectional area of the adsorbate molecule, m^2, and

S = adsorbent surface area, m^2/g

The cross-sectional area of the molecule can be calculated using the following expression employed by Emmett and Brunauer[14]:

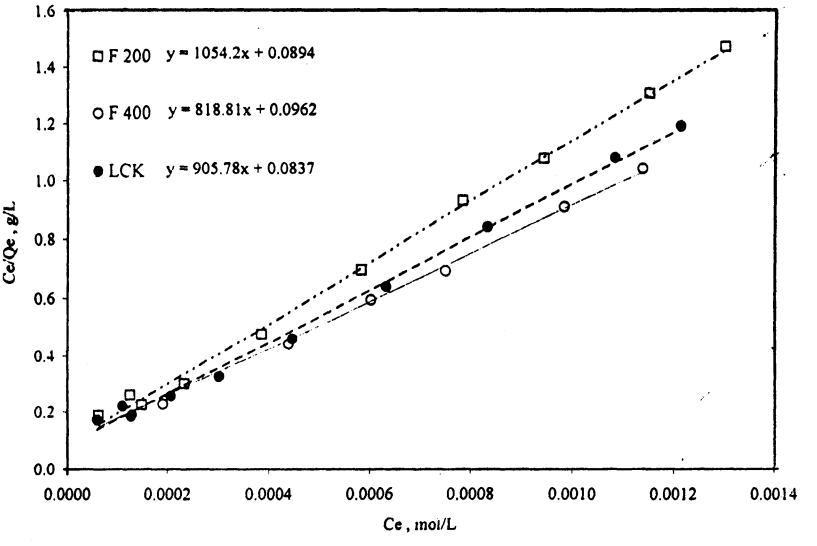

Fig. 4. Langmuir adsorption isotherms of *m*-nitrophenol on different grades of GAC

$$A = 3.464(M/4\sqrt{2}\,N\rho)^{2/3} \quad (5)$$

Where, M = molecular weight of the adsorbate,
ρ = density of the adsorbate (1.48 g/cm^3), and
$A = 32 \times 10^{-20}$ m^2 for *m*-nitrophenol.

The Langmuir isotherm constants, adsorbent surface area and the ratio of adsorbent surface area obtained from adsorption isotherm of *m*-nitrophenol and N_2-BET are summarised in Table-5

Adsorption kinetics: A simplified interpretation of the kinetic data based on Langmuir theory[10] has been used. Rate was expressed as a function of directly measurable system variable, the fluid phase adsorbate concentration. Rate constant found in this manner is purely phenomenological depending upon the rates of adsorption and diffusion. The individual processes like adsorption, desorption and molecular diffusion are all coupled together and represented by the overall rate constant.

Langmuir theory assumes that the rate of adsorption is proportional to the product of adsorbate concentration in the fluid phase and the fraction of the vacant adsorbent surface. The fraction of the surface covered by the adsorbate, Q, will be proportional to the decrease in fluid phase adsorbate concentration; thus

$$dQ/dt = k_a C_t(1 - Q) - k_d Q \quad (6)$$

and

$$Q = f(C_0 - C_t) \quad (7)$$

where, k_a and k_d are adsorption and desorption rate constants. C_0, C_t and C_e are the fluid phase adsorbate concentrations at zero, time t and at equilibrium

respectively, f is a constant. Substituting eqn. (2) in eqn. (1) and solving the resultant equation by applying the concept of steady state gives the final rate expression

$$\ln [(C_t - C_e) /(C_t + a)] = -k_a C_a t + \ln [(C_0 - C_e) /(C_0 + a)] \quad (8)$$

where $a = (C_0/bC_e)$ and $b = k_a /k_d$, the Langmuir constant.

The adsorption kinetic data for all the GAC-MNP systems were fitted into Eqn. (8) and was subjected to linear regression analysis to get the values of

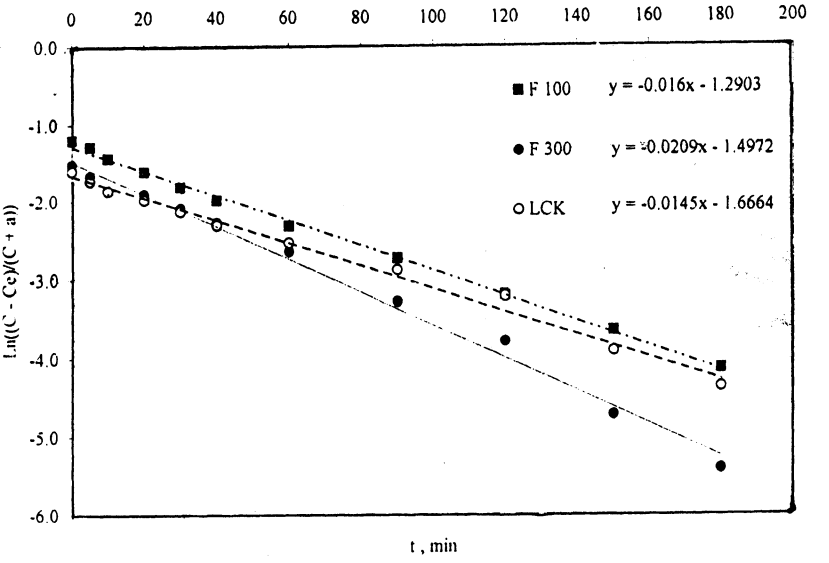

Fig. 5. Adsorption kinetics-plot of *m*-nitrophenol on various adsorbents

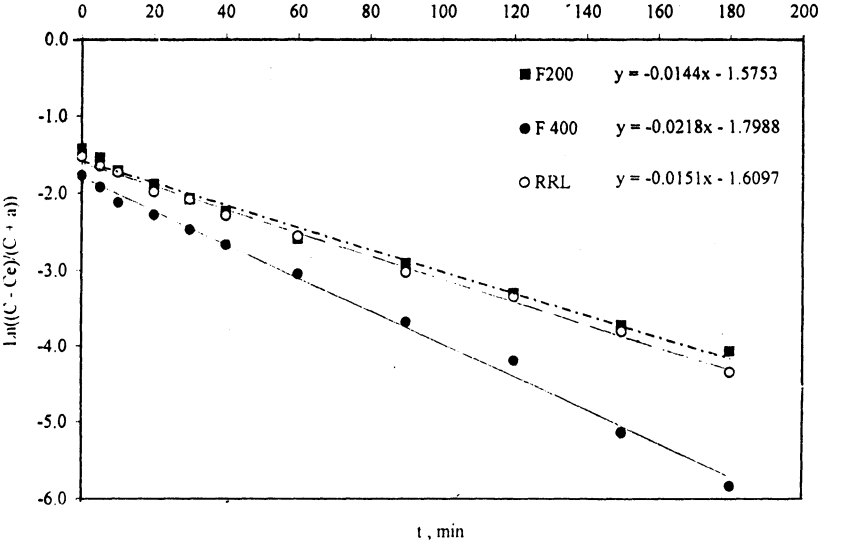

Fig. 6. Adsorption kinetics-plot of *m*-nitrophenol on various adsorbents

TABLE-5
LANGMUIR ADSORPTION ISOTHERM AND KINETIC CONSTANTS FOR VARIOUS MNP-GAC SYSTEMS

Adsorbate : *m*-nitrophenol, m.w. = 139.11, solubility in water at 30°C = 0.097 mol/L,
T = 30°C, pH = 6.9–7.1, GAC particle size = 12 × 16 mesh, A = 32 A^2

No.	Adsorption isotherm							Adsorption kinetics				
	GAC	Slope	Intercept	Q^o, mol/g	b	S_{MNP}, m^2/g	$S_{MNP}/S_{N_2,BET}$	Slope	Intercept	C_e, mol/L	k_a, min^{-1}	k_d, min^{-1}
1	F-100	1227.1	0.0788	0.00081	15572.3	157.1	0.1868	-0.0160	-1.2903	0.000042	380.95	0.024
2	F-200	1054.2	0.0894	0.00095	11791.9	182.8	0.2216	-0.0144	-1.5753	0.000038	378.95	0.032
3	F-300	889.7	0.0801	0.00112	11106.7	216.6	0.2233	-0.0209	-1.4972	0.000031	674.19	0.061
4	F-400	818.8	0.0962	0.00122	8511.5	235.4	0.2359	-0.0218	-1.7988	0.000026	838.46	0.099
5	RRL	923.5	0.0907	0.00108	10181.6	208.7	0.2319	-0.0151	-1.6097	0.000030	503.33	0.049
6	LCK	905.7	0.0837	0.00110	10821.0	212.8	0.2076	-0.0145	-1.6664	0.000034	426.47	0.039

adsorption and desorption rate constants. The linear regression coefficient values were above 0.98 for all the adsorbate-adsorbent systems. The k_a and k_d values are reported in Table-5.

Monolayer capacity of various grades of adsorbents for a particular adsorbate

Estimation of the specific surface area of an adsorbent is conventionally based upon measurements of the monolayer capacity Q° of the adsorbent for a selected solute having a well accepted molecular cross-sectional area. Since values of Q° were readily obtained from Langmuir plots (Table-5), it is possible to evaluate the adsorption performance of various adsorbents used. The cross-sectional area of phenol molecule is well established[12] and is taken as 52.2 $Å^2$. The MNP-BET surface area values for all the adsorbents are only about 20–24% of their reported N_2-BET surface area values. This clearly indicates that the finer pores are not accessible to the larger *m*-nitrophenol molecule (32 $Å^2$) as compared to the much smaller nitrogen molecule (16.2 $Å^2$). The pore size distribution measurements also corroborate these observations as more than 97% adsorbent surface area exists in the micropores below 35 Å in radius.

The monolayaer capacity of Filtrasorb grade of carbons is in the order F-400 > F-300 > F-200 > F-100 and from amongst the two coconut shell based carbons LCK shows a higher capacity than RRL. This is in accordance with their N_2-BET surface areas reported in Table-1. On the basis of the monolayer capacities one can conclude that F 400 is more suitable for scavenging organic pollutants from water. Although LCK has very large N_2-BET surface area, its MNP-BET surface area is lesser than F-400 which suggests that the coconut shell based carbons LCK and RRL have a greater proportion of finer pores not accessible to the larger phenol molecules. Further, the lower adsorption capacities of F-100 and F-200 are justified as they have lower N_2-BET surface area and are basically meant for gas phase adsorption and have very fine porous structure (as per the manufacturer's manual).

Rate of adsorption of MNP on various grades of adsorbents

The adsorption rate of MNP was found to be much higher for bituminous coal based GAC samples as compared to the coconut shell based adsorbents. This is because of the fact that the bituminous coal based carbons have wider pore size distribution and higher surface area with lot of cracks and cavities in its structure which favours the diffusion of the adsorbate species. Filtrasorb-300 and Filtrasorb-400 show the highest adsorption rate for m-nitrophenol.

Conclusions

This investigation on evaluation of adsorbents prepared from different sources has led to some important conclusions as stated below.

1. Pore size distribution (PSD), scanning electron microscopy (SEM), fourier

transform infrared spectroscopy (FTIR) and proximate and ultimate analysis show that the source material used for preparation of GAC has significant effect on its pore structure, surface texture and characteristic resistance to fragmentation and its adsorption capacity. Bituminous coal based GAC shows high ash content and loosely packed rough surface having a lot of cracks and crevices, irregular protrusions. The pores are widely dispersed pores and these carbons have high pore volume. The coconut shell based GAC samples have low ash content and low pore volume. These GAC samples exhibit uniformly dispersed and finer pores, well connected by solid mass. The presence of various acidic groups on the adsorbent surface formed during the activation process is corroborated by FTIR spectra. The low pore volume and high particle density of RRL sample also supports the above observation.

2. FTIR spectra show presence of various carbon-oxygen complexes on granular activated carbon surface which makes the surface slightly polar. Significant presence of free —OH stretch vibration of phenols around 3500 cm^{-1}, asymmetric and symmetric C—H stretch vibrations around 2868 cm^{-1}, asymmetric O=C=O stretch vibrations of CO_2 adsorbed in pores around 2347 cm^{-1} and C—O stretch vibration (phenol, —COO—) around 1200 cm^{-1} were observed in these carbons. Similarly C=O stretch vibrations around 1735 cm^{-1}, methylene vibrations around 1644 cm^{-1} were also present.
3. The experimental isotherm data did not adhere completely to either Freundlich or Langmuir models over the complete adsorbate equilibrium concentration range. However, the data could be fitted well to either model if one is selective in the equilibrium concentration range to be used in the analysis. These results clearly indicate that while using the Freundlich and Langmuir constants reported in literature for various adsorbates, due consideration must be given to the limitations of extrapolating these equation constants to other concentration ranges and experimental conditions.
4. The adsorption equilibrium isotherm data in the micromolar concentration range such as those used in the present work and which is more relevant to wastewater treatment, the B.E.T. equation and Langmuir equation give identical results.

ACKNOWLEDGEMENTS

Authors are thankful to Director-in-Charge and Dr. G.S. Natarajan, Professor and Head of the Department of Chemistry, Laxminarayan Institute of Technology, Nagpur University, Nagpur, for providing the necessary facilities to carry out this work. The first author (S.S.S.) is also thankful to Principal, Dr. Tidke and Dr. A.B. Bhake, Head of the Department of Applied Chemistry, Yashwantrao Chavan College of Engineering, Wanadongri, Nagpur, for their encouragement and cooperation.

REFERENCES

1. J. Van Driel, A. Capelle and F. de Vooys (Ed.), Activated carbon: A Fascinating Material, Norit N.V., Amersfoort (The Netherlands), pp. 40–57 (1983).
2. M. Modell, R.P. de Filippi and V. Krukonis, in: M.J. McGuire and I.H. Suffet (Eds.), Activated Carbon Adsorption of Organics from Aquous Waste, Vol. I, Ann Arbor Sci., Ann Arbor (Michigan) (1980).
3. Toshiro Otowa, Yutaka Nojima and M. Itoh, in: M. Douglas Le Van (Ed.), "Activation mechanism, surface properties and adsorption characteristics of KOH activated high surface area carbon", The Fundamentals of Adsorption (Proceedings of the 5th International Conference on Fundamentals of Adsorption) pp. 709–716 (1996).
4. R.G. Peel, A. Benedek and C.M. Crowe, *J. AIChE*, **27**, 28 (1981).
5. W.J. Weber, Physico-chemical Processes for Water Quality Control, Wiley-Interscience, New York (1972).
6. S.D. Faust and O.M. Aly, Adsorption Processes for Water Treatment, Butterworth Publishers, pp. 168–170 (1987).
7. J. Van Driel, A. Capelle and F. de Vooys (Eds.), Activated Carbon: A Fascinating Material, Norit N.V., Amersfoort (The Netherlands), pp. 40–57 (1983).
8. R.M. Silverstein, G.C. Bassler, and T.C. Morril, Spectrometric Identification of Organic Compounds, 4th Edn., John Wiley & Sons, New York, p. 112 (1981).
9. M.L. Studebaker and R.W. Rinehart (Sr.), Infra-red Studies of Oxygen Containing Groups on the Surface of Carbon Black (paper presented at the 10th Biennial Conference on Carbon, Bethlehem, Pennsylvania, 27 June–2 July 1971).
10. G.K. Bharat, M.K.N. Yenkie and G.S. Natarajan, in: M. Douglas Le Van (Ed.), Influence of Physico-chemical Characteristics of Adsorbent and Adsorbate on Competitive Adsorption Equilibrium and Kinetics, The Fundamentals of Adsorption (Proceedings of the 5th International Conference on Fundamentals of Adsorption, Kluwer Academic Publishers, pp. 91–100 (1996).
11. V.W. Uhl and J.B. Grey, Mixing: Theory and Practice, Vol. I, Academic Press (1966).
12. M.K.N. Yenkie and G.S. Natarajan, *Separation Sciene and Technology*, **28**, 1177 (1993).
13. ———, *Sep. Sci. & Technol.*, **26**, 661 (1991).
14. K.L. Kapoor, A Text Book of Physical Chemistry, Vol. 4, McMillan India Ltd., pp. 449-495 (1985).

(*Received*: 14 January 2002; *Accepted*: 15 February 2002) AJC-2625